TECHNICAL TRANSACTIONS | CZASOPISMO TECHNICZNE
CIVIL ENGINEERING | BUDOWNICTWO
1-B/2015

KAMIL SŁOWIŃSKI*, WALTER WUWER**

EXPERIMENTALLY AND ANALYTICALLY BASED SHAPING OF A BUILT-UP COMPRESSION BAR WITH DEFORMABLE JOINTS OF THE BRANCHES

KSZTAŁTOWANIE NA DRODZE DOŚWIADCZALNEJ I ANALITYCZNEJ ŚCISKANEGO PRĘTA ZŁOŻONEGO Z ODKSZTAŁCALNYMI POŁĄCZENIAMI GAŁĘZI

Abstract

This paper presents the course and results of a research programme aimed at the determination of the design buckling resistance of an axially compressed RHS column strengthened using two shorter U-sections. Connections of the tube and the channel branches were fabricated using BOM blind fasteners. Results of the experimental tests demonstrated the satisfactory efficiency of the performed strengthening of the tubular bar. Parametric analyses performed based on the validated theoretical model allowed the identification of the key factors influencing the effectiveness and economic efficiency of the strengthening process.

Keywords: *strengthening*, *buckling*, *built-up bars*, *flexible lap joints*

Streszczenie

W artykule przedstawiono przebieg i wyniki programu badawczego, którego celem było określenie obliczeniowej nośności wyboczeniowej ściskanego osiowo pręta o przekroju rurowym prostokątnym, wzmocnionego za pomocą dwóch krótszych gałęzi ceowych. Połączenia gałęzi rurowej i ceowych wykonano przy użyciu łączników jednostronnych BOM. Wyniki badań wykazały zadowalającą skuteczność wzmocnienia. Analizy parametryczne wykonane przy użyciu modelu teoretycznego umożliwiły identyfikację kluczowych czynników wpływających na skuteczność i efektywność ekonomiczną procesu wzmocnienia.

Słowa kluczowe: *wzmacnianie*, *wyboczenie*, *pręty złożone*, *podatne połączenia zakładkowe*

DOI: 10.4467/2353737XCT.15.083.3883

* Ph.D. Eng. Kamil Słowiński, Department of Geomechanics, Civil Engineering and Geotechnology, Faculty of Mining and Geoengineering, AGH University of Science and Technology.

** Ph.D. D.Sc. Assoc. Prof. Walter Wuwer, Faculty of Architecture, Civil Engineering and Applied Arts Faculty, Katowice School of Technology.

1. Introduction

Steel hollow sections are widely used in the building industry, mainly due to their beneficial strength parameters. An extensive area of application for tubular sections are lightweight roof lattice girders (Fig. 1). If a building changes its function and the loads increase, a problematic issue may be the strengthening of the tubular bars of the truss, e.g. axially compressed diagonals made from rectangular hollow section (RHS), (Fig. 1). In addition, postulates of sustainable development in building require the strengthening process to be characterized by low energy expenditure.

Fig. 1. Lattice girders made from closed and open steel sections

Currently, a rapid development of methods of strengthening tubular bars using CFRP composites, which are glued to the walls of the strengthened bar, may be observed [1–4]. However, it should be noted that the process of strengthening using CFRP composites requires substantial amounts of work, mainly due to the necessity to ensure good adhesion of the composite to the surface of the strengthened element [5]. Another popular method to improve the stability conditions of the member in compression consists of welding shorter steel strengthening branches to the strengthened bar [6]. However, welding, due to it being an energy consuming process, does not fit into the framework of a sustainable building. The application of bolted joints – with the desired structural properties – is limited to the joint with access from both sides. The use of easy to install, self-tapping and self-drilling screws, blind rivets or innovative blind fasteners [7, 8] is, in turn, limited due to their low shear resistance and thus, there is a need to use a large number of fasteners in the fastening. These fasteners are therefore used mainly in the connections of walls of thickness not exceeding 3 mm [9–13]. Against this background, the attention may be paid to the blind fasteners BOM (blind, oversize, mechanically locked) [14] having the shear resistance comparable to the bolts of grade 10.9. BOM fasteners are mainly used in the automobile industry and occasionally in civil engineering (Fig. 2). The works of Wuwer [15–17]

and Swierczyna [18–20] revealed that BOM fasteners may be used as an alternative to standard bolts in the lap joints in the nodes of the lightweight latticed frames made from both open and closed steel sections. The tests revealed significant reserves in the strength, stiffness and ductility of the studied connections working in the bearing. It should be noted that the bearing action in connections was not taken into account in existing applications of the BOM fasteners.

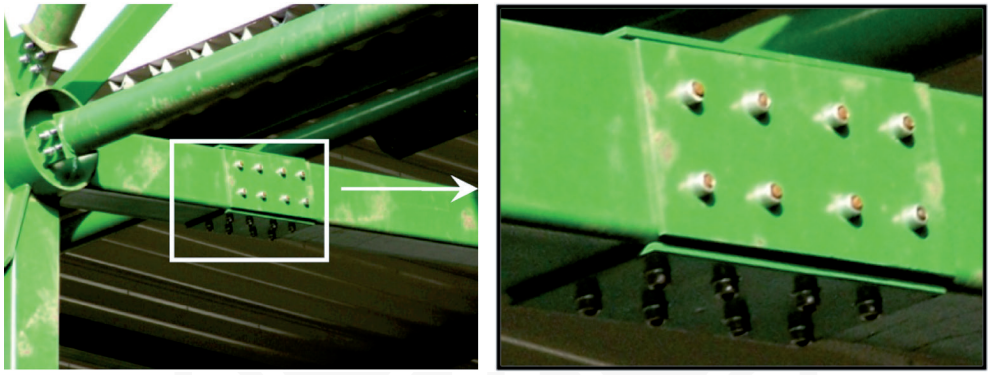

Fig. 2. Splice with blind fasteners BOM in the bottom chord of the truss made of tubular sections

The research performed by Wuwer and Swierczyna provided the basis to initiate a research programme aimed at the experimental and analytical study of axially compressed bars made from RHS, symmetrically strengthened by two shorter channel branches [21]. The article presents the results of experimental and theoretical studies that provide answer to the question of whether blind fasteners (BOM) may be an effective alternative to standard bolts in joints of walls of strengthened tubular bars and strengthening branches of open cross--sections.

2. Investigation programme

Within the first stage of the research programme, experimental tests of single lap joints with BOM fasteners in shear had been foreseen. The tests were aimed at the determination of the basic structural properties of the joints in working conditions similar to those for the connections of the branches in the built-up bars (intended for research in the second stage of the research programme).

The second stage of the programme covered tests of five identical columns in compression, composed of interconnected: tubular bar and two shorter strengthening branches The aim of the study was to determine the buckling resistance of the observed built-up bars with connections of the branches made using BOM fasteners.

The third stage of the study incorporated the verification of the theoretical model describing the structural behaviour of the tested built-up bars.

Finally, the fourth stage included parametric analyses performed based on the validated theoretical model. The purpose of the analyses was to identify the key factors influencing the effectiveness and economic efficiency of the strengthening process.

3. Inventory of steel sections and material tests

An inventory of sections RHS100×60×4 and U30/60/30×4, intended for installation in test elements was performed prior to the experimental tests. Measurements of the cross-sectional geometry of the RHS revealed for the webs (side B and C in Fig. 3) both bow imperfections of a maximum value of 0.5 mm towards the interior of the cross-section and the difference in the thickness t (Fig. 4). The basic geometrical properties for the sections are presented in Table 1.

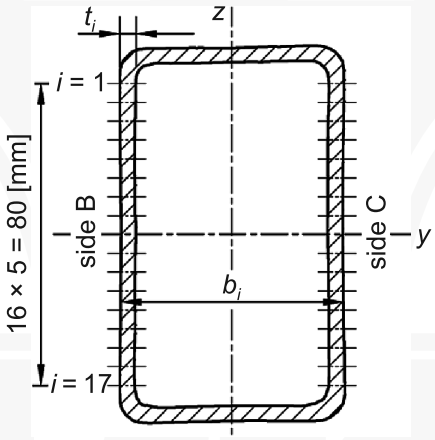

Fig. 3. Cross-section of RHS100×60×4 with measurement points

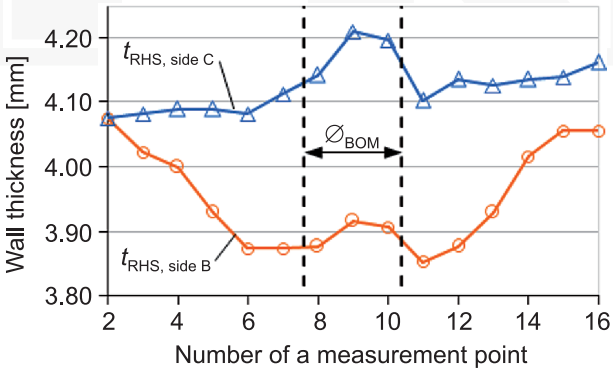

Fig. 4. Distribution of thickness of the walls B and C for RHS100×60×4

Table 1

Cross-sectional properties of sections

Section	A [cm^2]	t [mm]	$t_{RHS,side\ B}$ [mm]	$t_{RHS,side\ C}$ [mm]
RHS100×60×4	12.27	4.12	4.06	4.16
U30/60/30×4	4.27	3.98	–	–

For the material tests, four rectangular pieces were extracted from the webs of the tube as well as the channel section (Fig. 5). The destination shape of the specimens, according to [22], was obtained using the water jet cutting method. Tensile tests were performed using the Zwick Z/100 machine (Fig. 6). Measured mechanical properties of the specimens, determined according to [22], are presented in Table 2.

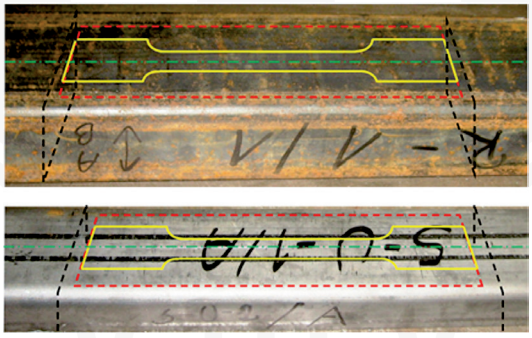

Fig 5. Locations for the extraction of specimens from tubular (above) and channel (below) sections

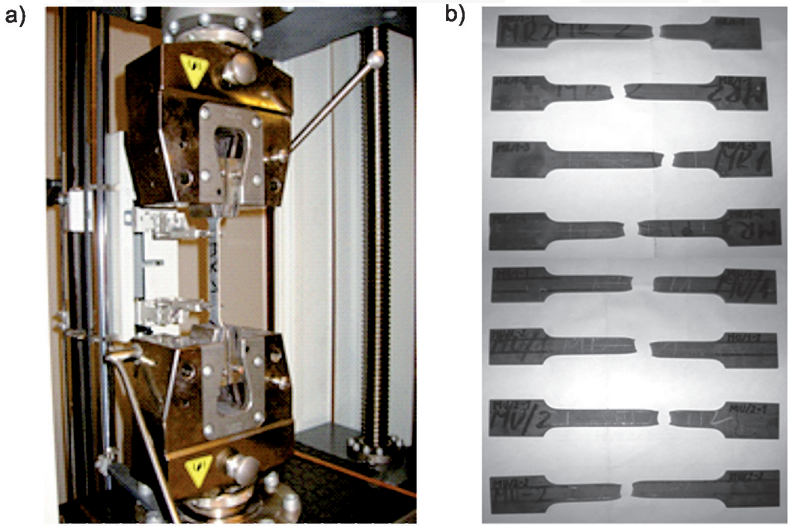

Fig. 6. Tensile tests: a) test set-up, b) specimens after tests

Table 2

Tensile tests results

Section	Steel	R_{eH} [MPa]	R_{eL} [MPa]	R_m [MPa]	E [MPa]
RHS100×60×4	S355J2H	402.63	372.23	528.45	203874.5
	standard deviation	6.11	1.99	2.72	3992.38
U30/60/30×4	S355	407.11	392.47	545.96	189928.7
	standard deviation	7.92	9.85	2.49	6398.23

4. Shear tests of joints

4.1. Construction of test elements

The experimental tests covered six identical test elements subjected to axial tension. Each of the elements was composed of RHS100×60×4 and two branches U30/60/30×4 (Fig. 7). The abutting walls of the sections were interconnected using two BOM-R16-4 fasteners [14] (Fig. 8). The specimens were equipped with short sections of the tube and the channels, in order to increase the bearing capacity of the anchorage in the testing machine (Fig. 7).

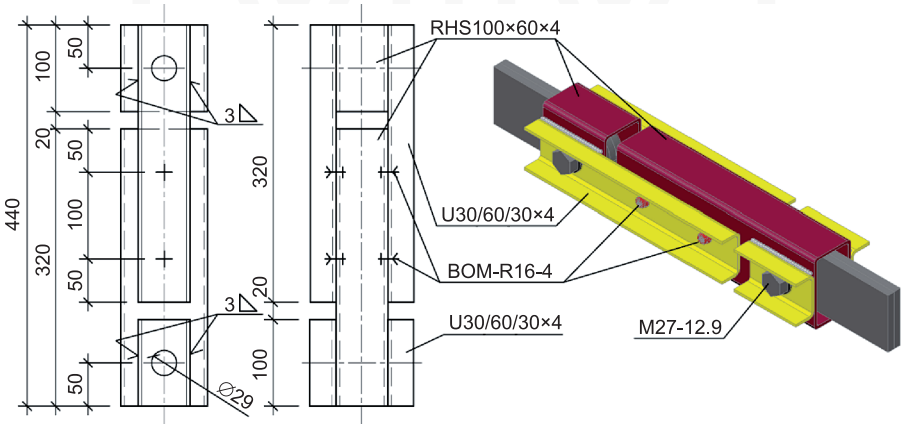

Fig. 7. Construction and dimensions (in millimetres) of test elements

Fig. 8. BOM-R16-4 fastener

4.2. Assembly of test elements

The BOM-R16-4 fasteners were installed in drilled holes with a nominal diameter of 14 mm. The measurement performed before installation revealed positive deviations of diameters with values of up to 9.5% of the nominal diameter. Installation of the BOM fasteners was performed using the installation tool (Fig. 9) which upsets the sleeve of the fastener, forming a head on the blind side and the locking groove on the accessible side (Fig. 10) [14].

Fig. 9. Merging the channel section with the tubular section

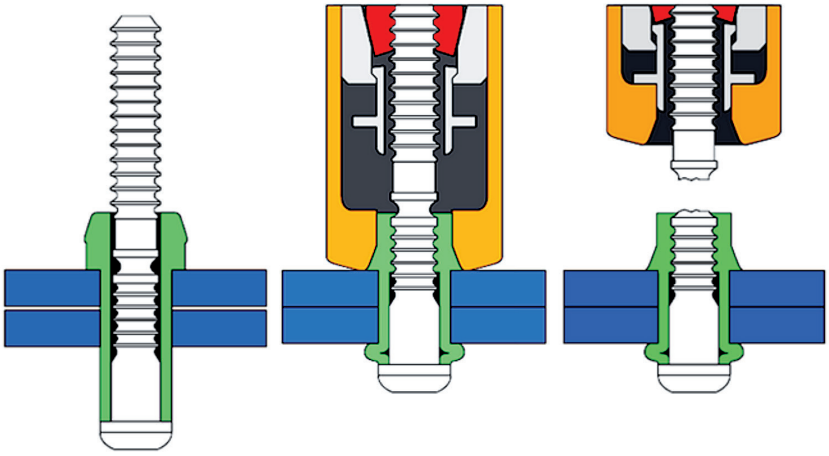

Fig. 10. Installation sequence of a BOM fastener [14]

4.3. Test procedure and measurement equipment

The test elements were subjected to axial tension in a hydraulic testing machine (Fig. 11). The load was applied in increments of 1 kN/min until the occurrence of significant deformations in the fastening, after which the test elements were unloaded.

By using four electronic displacement transducers (DT) (Fig. 11), the mutual displacements of the walls of the interconnected tube and the channel section were measured (two DTs were applied for each of the two connections).

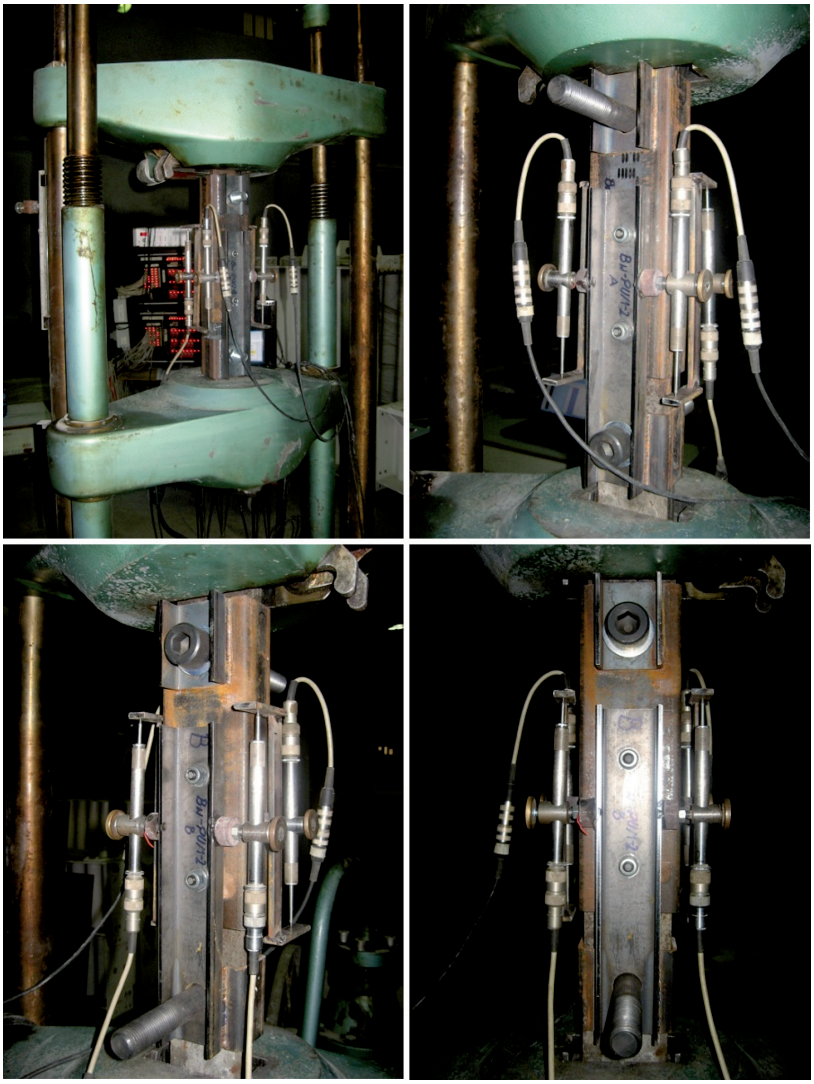

Fig. 11. Shear test set-up

4.4. Shear test results

4.4.1. Static equilibrium paths and failure modes

Fig. 12 shows the measured relationships between the shear force F acting on a single fastener (one-fourth of the tension force loaded the tested element) and the deformation v on the load direction. The magnitudes of the deformation v are the average values from the results of measurements recorded for each of the six tested elements, labelled as S-1 to S-6. As can be seen (Fig. 12), in the first phase of loading, i.e. for $F \leq 45$ kN, relationships

$F - v$ remained essentially linear. With increasing load, the gradual degradation of joint stiffness accompanied by tilting of the fasteners on the load direction was observed. Above the level of the shear force $F \approx 60$ kN, a significant increase in deformation v was recorded. This increase was accompanied by further tilting of fasteners, noticeable plastic ovalisation of holes and also, permanent deformations of the interconnected walls from the contact plane (Fig. 13). The specimens were unloaded at the deformation level $v \approx 15$ mm (Fig. 12).

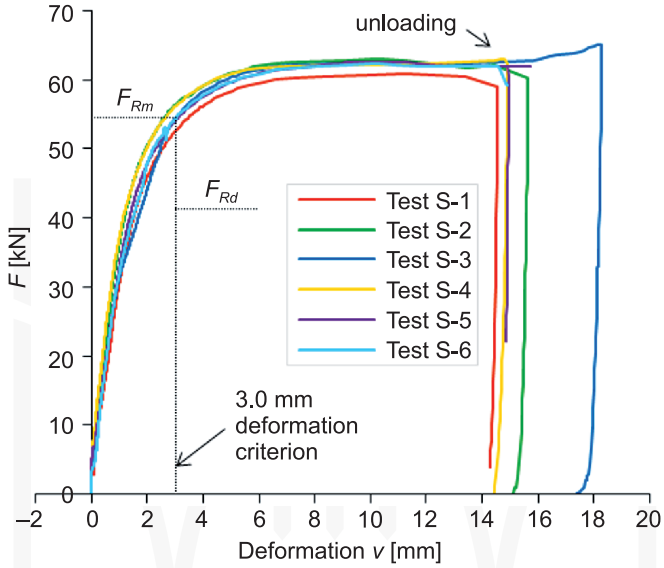

Fig. 12. Relationships $F - v$ for tested elements (average for two connections

Fig. 13. Typical failure mode of the specimen after unloading

4.4.2. Design bearing resistance of connections

The design bearing resistance of the tested connections (1) in accordance with [23] was determined based on the deformation criterion of 3 mm by calculating: the characteristic resistance (2), the mean value (3) and the adjusted value (4), and also standard deviation (5), using the formulae:

$$F_{Rd} = \frac{F_{Rk}}{\gamma_M}, \tag{1}$$

$$F_{Rk} = F_{Rm} - k \cdot s, \tag{2}$$

$$F_{Rm} = \frac{F_{R,adj,1} + F_{R,adj,2} + \ldots + F_{R,adj,n}}{n}, \tag{3}$$

$$F_{R,adj,i} = \frac{F_{R,obs,i}}{\mu_R}, \tag{4}$$

$$s = \sqrt{\frac{1}{n-1}\sum_{i=1}^{n}(F_{R,adj,i} - F_{Rm})^2}, \tag{5}$$

where:

- k – characteristic fractile factor according to [24],
- n – number of test elements,
- $F_{R,obs,i}$ – measured test result for test i,
- γ_M – partial factor for resistance according to [23] and [25],
- μ_R – adjustment coefficient (calculations were performed for the measured values).

The results of the statistical evaluation according to formulae (1)–(5) are shown in Table 3.

Table 3

Results of statistical evaluation for design resistance F_{Rd}

F_{Rm} [kN]	s [kN]	k	μ_R	F_{Rk} [kN]	γ_M	F_{Rd} [kN]
54.59	1.37	2.18	1.0	51.61	1.25	41.3

For the measured relationships $F - v$, using the least squares method, the resulting analytical curve was determined of the form (Fig. 14):

$$F = 62.29(1 - e^{-0.7391\,v}). \tag{6}$$

For the resulting curve, the instantaneous stiffness k_v corresponding to deformation: v = 1 mm – assumed as an upper boundary of the elastic action of the fastening, and v = 3 mm – according to the adopted deformation criterion, were developed (Table 4, Fig. 14). Based on the obtained results, it may be concluded that due to the relatively high degradation of stiffness k_v, the tested fastenings were strenuous at the plastic range at the level of deformation v = 3 mm.

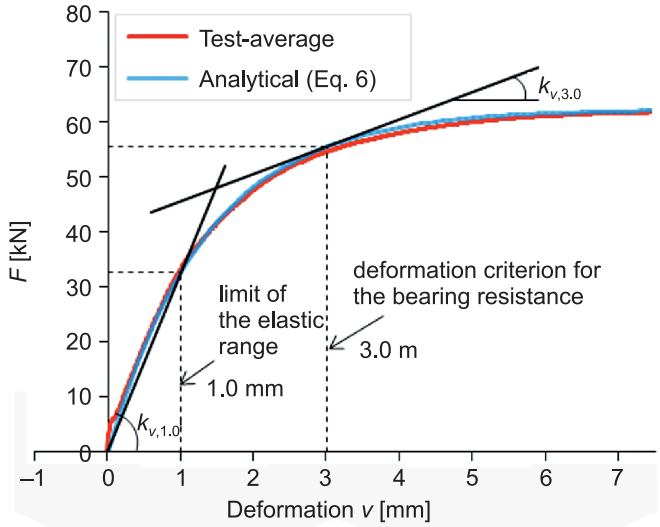

Fig. 14. Instantaneous stiffness of fastening at the level of deformation: $v = 1.0$ mm and $v = 3.0$ mm

Table 4

Instantaneous stiffness for tested fastening

	$k_{v,1.0}$	$k_{v,3.0}$
[kN/mm]	32.54	5.01
[%]	100%	15.4

4.4.3. Assessment of results

Fig. 15 shows the bi-linear relations $F - v$ determined for the tested connections with fasteners BOM-R16-4 and analogous connections with bolts M16 of grade 8.8. The bearing resistance and the stiffness of the bolted connection was established according to [25] (Table 5). As it can be seen, connections with BOM fasteners provide greater stiffness than

Table 5

Design stiffness for connections with BOM fasteners and M16 standard bolts according to [25]

Fastener	Bolt M16-8.8	BOM-R16-4
k_v [kN/mm]	19.75	28.07
[%]	100	142.1
F_{Rd} [kN]	64.4	41.3
[%]	100	64.1

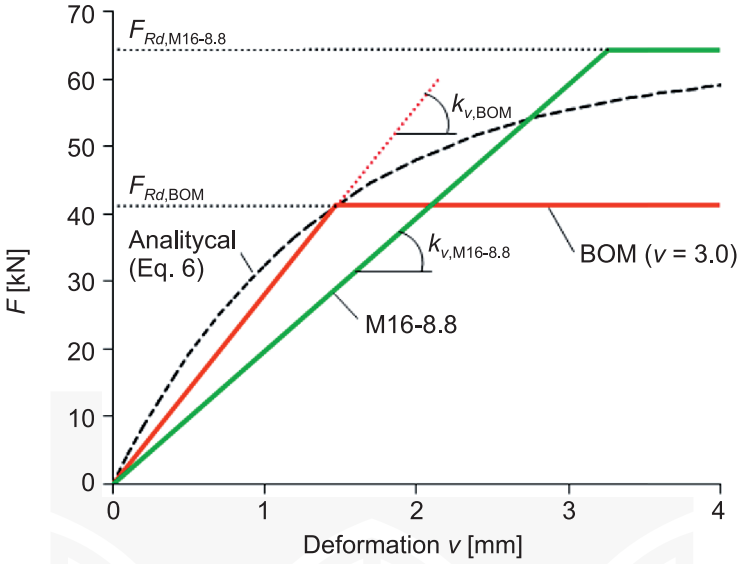

Fig. 15. Bi-linear relationships F-v for connections with BOM fasteners and M16-8.8 bolts

the bolted connections. It should be noted that the relationship $F - v$ for the bolted connection does not include a possible slip in the fastening (for connections with BOM fasteners, the slip does not occur [21]). However, it can be seen that design bearing resistance of the connections with BOM fasteners is noticeably smaller than those for bolted connections.

5. Tests of built-up columns

5.1. Construction of test elements

The second stage of the research programme covered tests of five identical three-branched, pin-ended columns subjected to axial compression. The main bar (intended for strengthening) to which the compressive force was applied at the ends was made from RHS100×60×4 with a length of 3000 mm (Fig. 16). Each of the two channel branches U30/60/30×4 (foreseen as strengthening branches) with a length of 2960mm was connected with a main tubular bar using eight BOM-R16-4 fasteners, uniformly spaced at 408mm (Fig. 16). Installation of the

Fig. 16. Three-branched column foreseen for test (before installation of BOM fasteners)

fasteners was performed using the installation tool (Fig. 17) – previously, this was also used for the assembly of specimens for shear tests. Pinned-end conditions and the axial transfer of compressive force to the column was provided by – performed with high precision – end fixtures (Fig. 18). The buckling length of the tested elements placed on the test stand was L = 3139 mm.

Fig. 17. Assembly of the branches of the built-up column

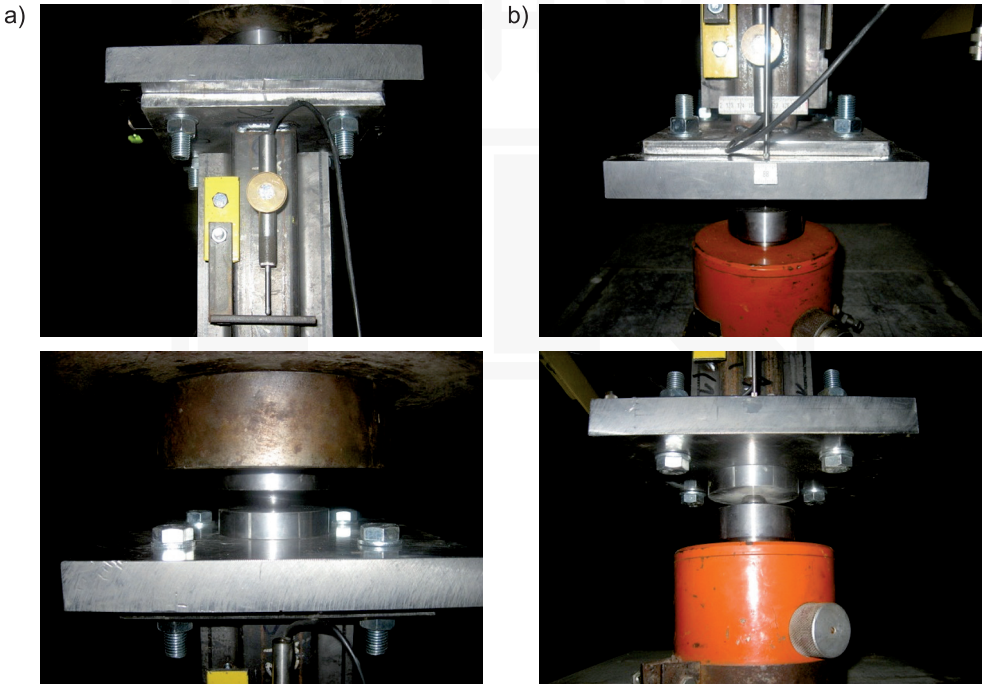

Fig. 18. End fixtures for tested columns: a) upper head, b) bottom head

5.2. Test procedure

The compression tests were performed using a hydraulic testing machine with loads range up to 1000 kN (Fig. 19a). The axial load was applied in increments of 10 kN/min [26], until the failure of the tested elements. During the test, strains of the walls of the tubular main bar were measured using stain gauges. Furthermore, by means of electronic displacement transducers (DT), the following measurements were recorded:

– lateral deflections normal to both principal axes of the built-up cross-section (at quarter points of the tested column), (Fig. 19b, c);
– mutual displacements between the interconnected walls of the tubular bar and channel branches (in the axis of each connection), (Fig. 19c);
– overall column shortening (Fig. 19d).

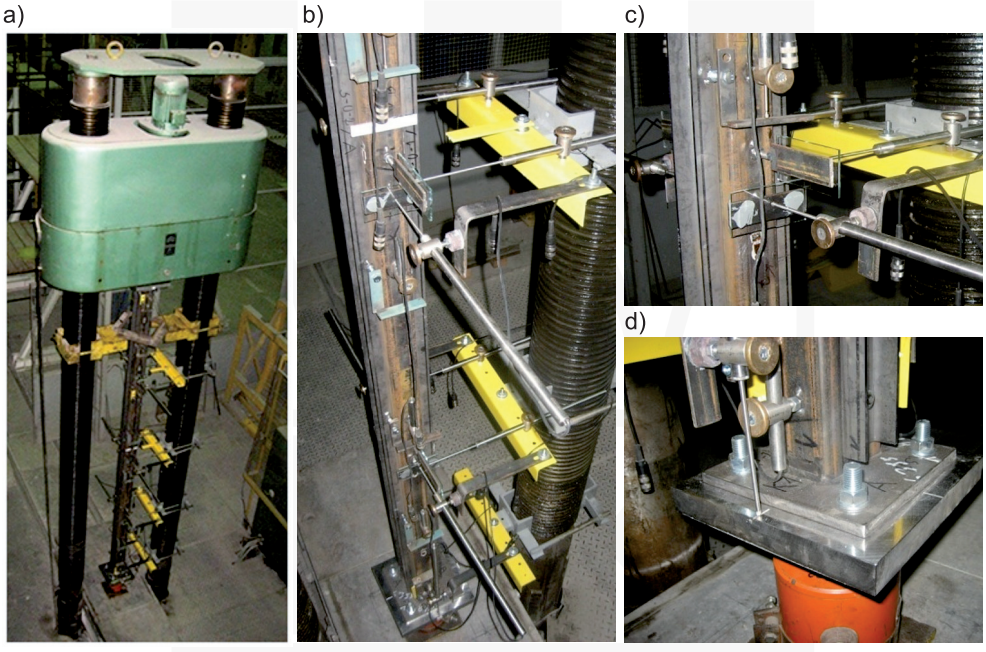

Fig. 19. Column test set-up: a) general view; b) and c) arrangement of DTs for measurement lateral deflections of the column and displacements between interconnected sections, respectively; d) instrumentation for recording overall shortening of the column

5.3. Column test results

5.3.1. Failure mode

The destruction of all the tested elements, labelled as Bz-1 to Bz-5, was as a result of their flexural buckling (Fig. 20) around the z axis of the built-up cross-section (Fig. 16). Figure 21 summarises the achieved relationships between the loaded axial force N and the

lateral deflection u_y (Fig. 21a) or u_z (Fig. 21b), i.e. measured in the *xy* plane or *xz* plane (Fig. 16) at the mid-length of the column (Fig. 19c).

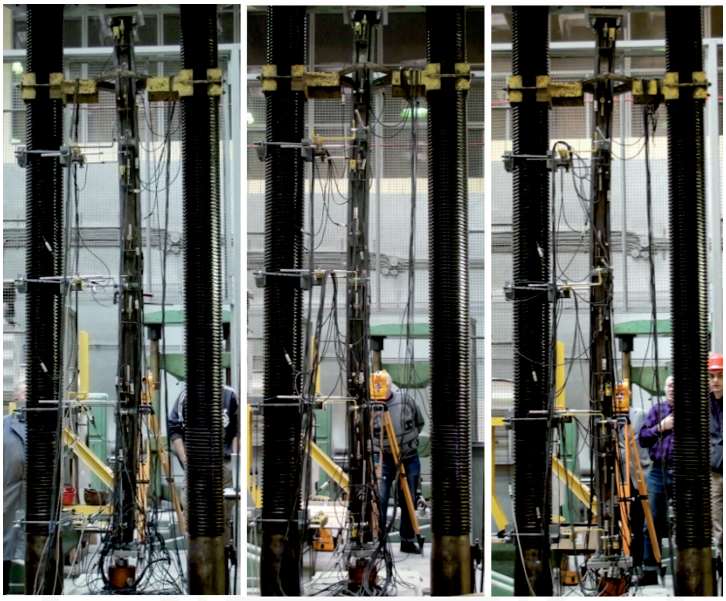

Fig. 20. Typical failure model of tested columns

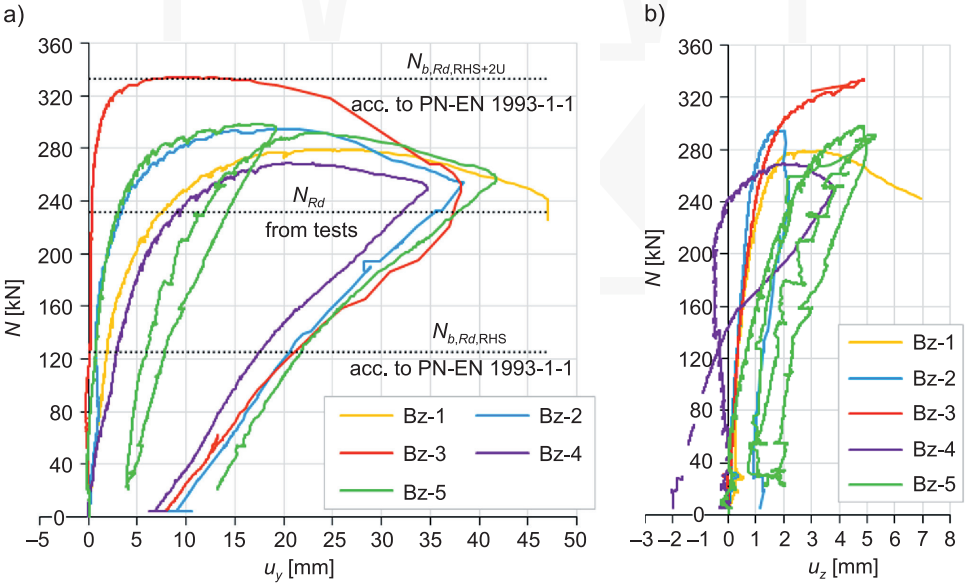

Fig. 21. Measured relationships load-lateral deflection: a) $N - u_y$, b) $N - u_z$

5.3.2. Design buckling resistance of built-up columns

It was assumed that for each tested column, the design criterion for the ultimate capacity will be determined by the lowest value of the axial force N, which is accompanied by:
- achievement of the buckling strength (N_{ult}) or
- yielding in extreme fibres of cross-section of the tubular main bar (N_{pl}) or
- achievement of the design bearing resistance by any connection of the branches.

The value of the N_{pl} was calculated based on the state of normal stresses in the most strenuous point along the length of the tubular bar. The normal stresses were calculated as the sum of the residual stresses, in accordance with [27] and the stresses determined on the basis of the strain gauge measurements. For each test element, the first yielding occurred in the walls of the tubular cross-section, on the concave side of the deflected (buckled) column, usually at the axis of the joint which was the nearest to the column's mid-point. The measured values of forces N_{ult} and N_{pl} are summarised in Tables 6 and 7. For the group of test elements, the average values of compressive stresses in the tubular cross-section under the load $N = N_{ult}$ constituted from 79% (in element Bz-4) to 93% (in element Bz-3) of the upper yield strength R_{eH} for the RHS material (Table 2).

The design buckling resistance N_{Rd} for tested columns was statistically determined based on the values of load N_{pl} (Table 7, Table 8), using equations (1) to (6) – in the formulae, symbol F was replaced with symbol N. The calculation results are presented in Table 9. As can be seen, the achieved design buckling resistance N_{Rd} constitutes approx. 185% of the buckling resistance of the tubular bar only, according to [28] (Fig. 21a). At the same time, the calculated resistance N_{Rd} constitutes approx. 70% of the buckling resistance of the theoretical built-up column with equal lengths of the three perfectly rigid interconnected branches, according to [27] (Fig. 21a). It should be noted that for each tested element, shear forces acting in the joints of the branches were lower than the design bearing resistance of those joints [21].

Table 6

Ultimate load N_{ult} for tested columns

Specimen	Bz-1	Bz-2	Bz-3	Bz-4	Bz-5
Measured value N_{ult} [kN]	278.85	294.6	333.81	269.11	298.48
Average value N_{Rm} [kN]	294.97				
Standard deviation s [kN]	24.75				
Coefficient of variation V	0.084				

Table 7

Load N_{pl} for tested columns

Specimen	Bz-1	Bz-2	Bz-3	Bz-4	Bz-5
Measured value N_{pl} [kN]	277.1	291.62	333.64	264.92	296.86
Average value N_{Rm} [kN]	292.83				
Standard deviation s [kN]	26.03				
Coefficient of variation V	0.089				

Table 8

Comparison of measured values of loads N_{ult} and N_{pl}

Specimen	Bz-1	Bz-2	Bz-3	Bz-4	Bz-5
Ratio N_{ult}/N_{pl}	1.01	1.01	1.0	1.02	1.01

Table 9

Results of statistical evaluation for the design buckling resistance N_{Rd}

N_{Rm} [kN]	s [kN]	k	μ_R	N_{Rk} [kN]	γ_M	N_{Rd} [kN]
292.86	26.03	2.33	1.0	232.1	1.0	232.2

6. Analytical solution

6.1. Computational model

The computational model describing the behaviour of the tested built-up columns was developed in the Wolfram Mathematica program [29]. A detailed description of the model is given in the work [21]. The model takes into account nonlinear geometric relationships for the built-up column, linear material characteristics and nonlinear relationships describing

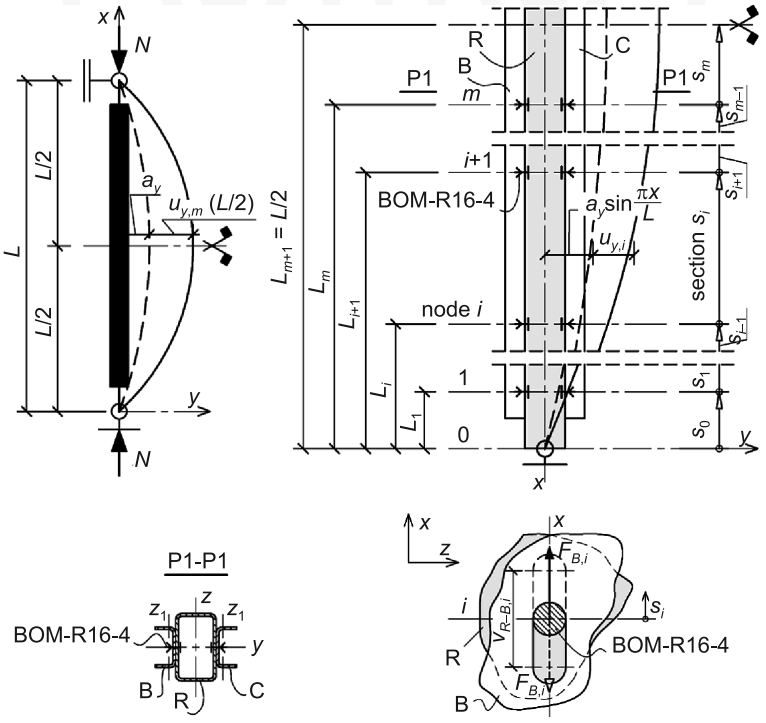

Fig. 22. Scheme of the computational model (description in the text)

the structural behaviour of joints of the branches. The model makes it possible to obtain: the axial force N loading the column; shear forces F_i acting in the joints of branches in nodes $i = 1 - m$ (Fig. 22); a lateral deflection in the xy plane at any point along the column length. Results may be achieved for given amplitudes of initial curvature – a_y and lateral deflection of the column under the load $N - u_{y,m}(L/2)$.

The solution, in the general form, for column buckling about z axis, is governed by the set of equations that are assigned to sections $s_0 - s_m$ (Fig. 22) along half of the column length:

– describing lateral deflection of the column axis (7)–(9) and the angle of the inclination of the tangent to this axis (10)–(11)

$$u_{y,0}(0) = 0, \tag{7}$$

$$u_{y,i-1}(L_i) = u_{y,i}(L_i), \tag{8}$$

$$u_{y,m}(L/2) = u_y, \tag{9}$$

$$u'_{y,i-1}(L_i) = u'_{y,i}(L_i), \tag{10}$$

$$u'_{y,m}(L/2) = 0; \tag{11}$$

– describing bending moments (12–13) and transverse forces (14–16)

$$EI_{\mathrm{RHS},z}u''_{y,0}(0) = 0, \tag{12}$$

$$(2EI_{U,z1} + EI_{\mathrm{RHS},z})u''_{y,i}(L_i) = -N\left[u_{y,i}(L_i) + a_y \sin\frac{\pi L_i}{L}\right] + w(N_{B,i} + N_{C,i}), \tag{13}$$

$$EI_{\mathrm{RHS},z}u'''_{y,0}(L_1) + Nu'_{y,0}(L_1) = (2EI_{U,z1} + EI_{\mathrm{RHS},z})u'''_{y,1}(L_1) + Nu'_{y,1}(L_1), \tag{14}$$

$$(2EI_{U,z1} + EI_{\mathrm{RHS},z})u'''_{y,i-1}(L_i) + Nu'_{y,i-1})L_i) = (2EI_{U,z1} + EI_{\mathrm{RHS},z})u'''_{y,i}(L_i) + Nu'_{y,i}(L_i), \tag{15}$$

$$(2EI_{U,z1} + EI_{\mathrm{RHS},z})u'''_{y,m}(L/2) + Nu'_{y,m}(L/2) = 0; \tag{16}$$

– linking the values of deformations v_i with the values of shear forces $F_{B,i}$ or $F_{C,i}$, occurring in joints of the branches B and R (17) or C and R (18)

$$\sum_i^m \int_{L_i}^{L_{i+1}} \Delta\varepsilon_{R-B,i}(x)\,dx = v_i(F_{B,i}), \tag{17}$$

$$\sum_i^m \int_{L_i}^{L_{i+1}} \Delta\varepsilon_{R-C,i}(x)\,dx = v_i(F_{C,i}); \tag{18}$$

where:

$$u_{y,0}(x) = C_{0,3}x + C_{0,4} - \frac{C_{0,1}\cos(k_{\mathrm{RHS}}x) + C_{0,2}\sin(k_{\mathrm{RHS}}x)}{k_{\mathrm{RHS}}^2} + \frac{a_y k_{\mathrm{RHS}}^2 L^2 \sin\left(\dfrac{\pi x}{L}\right)}{-k_{\mathrm{RHS}}^2 L^2 + \pi^2}, \tag{19}$$

$$u_{y,i}(x) = C_{i,3}x + C_{i,4} - \frac{C_{i,1}\cos(k_{\mathrm{RHS}+U}x) + C_{2,2}\sin(k_{\mathrm{RHS}+U}x)}{k^2_{\mathrm{RHS}+U}} + \frac{a_y k^2_{\mathrm{RHS}+U} L^2 \sin\left(\frac{\pi x}{L}\right)}{-k^2_{\mathrm{RHS}+U}L^2 + \pi^2}, \quad (20)$$

$$k^2_{\mathrm{RHS}} = \frac{N}{EI_{\mathrm{RHS},z}}, \quad (21)$$

$$k^2_{\mathrm{RHS}+U} = \frac{N}{2EI_{U,z1} + EI_{\mathrm{RHS},z}}, \quad (22)$$

where:

C_0, C_i – integration constants,
$EI_{\mathrm{RHS},z}$ – bending stiffness of the main tubular bar in the *xy* plane (Fig. 22),
$EI_{U,z1}$ – bending stiffness of the channel branch in the *xy* plane (Fig. 22),
$N_{B,i}$, $N_{C,i}$ – axial forces in the branches B and C, respectively, in section s_i,
w – distance between neutral axes of branches R and B or R and C,
$v_i(F_{B,i})$, $v_i(F_{C,i})$ – functions defining relationships between the values of deformation and shear force in the *i* joint of the branches B and R or C and R,
$\Delta\varepsilon_{R-B,i}$, $\Delta\varepsilon_{R-C,i}$ – functions describing the state of strains of branches B and R or C and R in the axis of *i* joint,

the other symbols are in accordance with Fig. 22.

7. Comparison of experimental and analytical results

The calculations were performed in three variants: CW1, CW2 and CW3, depending on the function describing the boundary conditions in the joints of the branches adopted in the analytical solution (Fig. 23):

– obtained from the shear tests: nonlinear C1 according to (6) or linear C2 according to the bi-linear curve shown in Fig. 15,
– C3 which linearly approximates the averaged measured relationships between shear force F_1 and deformation v_1 in the joint of the branches in node 1 (Fig. 22).

The amplitudes of the initial curvature of the built-up column (a_y) were taken in calculations in such a way as to achieve the best possible fit of analytical and experimental curves. As can be seen (Fig. 24), the critical load for the perfectly straight column ($a_y = 0$) calculated in variants CW1 and CW2 was smaller, in many cases, than the value of the measured axial force N (Fig. 24a, b, c, e). The best approximation of the experimental results provide curves CW3 for the amplitudes a_y within the range from 0.48 mm (Fig. 24e) to 2.62 mm (Fig. 24d). The distinct behaviour of the test element Bz-3 (Fig. 24c) can be explained by unintentional partial rotational restraining of the column ends. Comparison of test results – averaged for elements Bz-1, Bz-2, Bz-4 and Bz-5, and analytical results – obtained for the average amplitude $a_y = L/2207 \approx 1.42$mm is presented in Fig. 25. On the basis of the course of both curves, it may be concluded that the analytical solution provides satisfactory approximation of the experimental results.

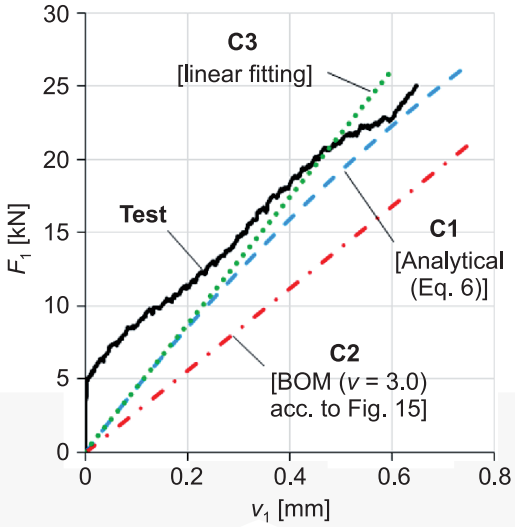

Fig. 23. Relationships $F_1 - v_1$ adopted in the analytical solution

8. Parametric analysis

Using the theoretical model, a parametric analysis was performed adopting linear stiffness function of the joints C3 (Fig. 23) and the averaged magnitude of the amplitude of initial curvature of the built-up column $a_y = L/2207$ in the calculations (Fig. 25).

The structural response of the built-up column was analysed in the case of:

– the change in cross-sectional dimensions of the channel branches at a constant number of connections (m = 4, Fig. 22) of the main tubular bar with each of the two channel branches – the continuous curves in Fig. 26,
– an increase in the number of joints of each of the two channel branches U30/60/30×4 with the tubular bar, from eight (m = 4) to sixteen (m = 8), twenty-four (m = 12), thirty-two (m = 16) and forty (m = 20) – the dashed curves in Fig. 26.

Calculations were carried out up to the moment when the normal stresses in any point of the tube cross-section were equal to the upper yield strength R_{eH} of the RHS material.

Form the performed parametric analysis it may be concluded that (see Fig. 26):

– an increase in the number of joints does not significantly raise the efficiency of strengthening (continuous curves); when doubling the number of joints from eight (m = 4) to sixteen (m = 8), the carrying capacity of the built-up column increases by approx. 9.5%; further doubling the number of joints (from m = 8 to m = 16) provides only a 5% increase in the carrying capacity,
– the carrying capacity for the built-up column with forty (m = 20) flexible joints of branches with BOM fasteners constitutes nearly 97% of the carrying capacity of the built-up column but with perfectly rigid joints (the dotted curve),

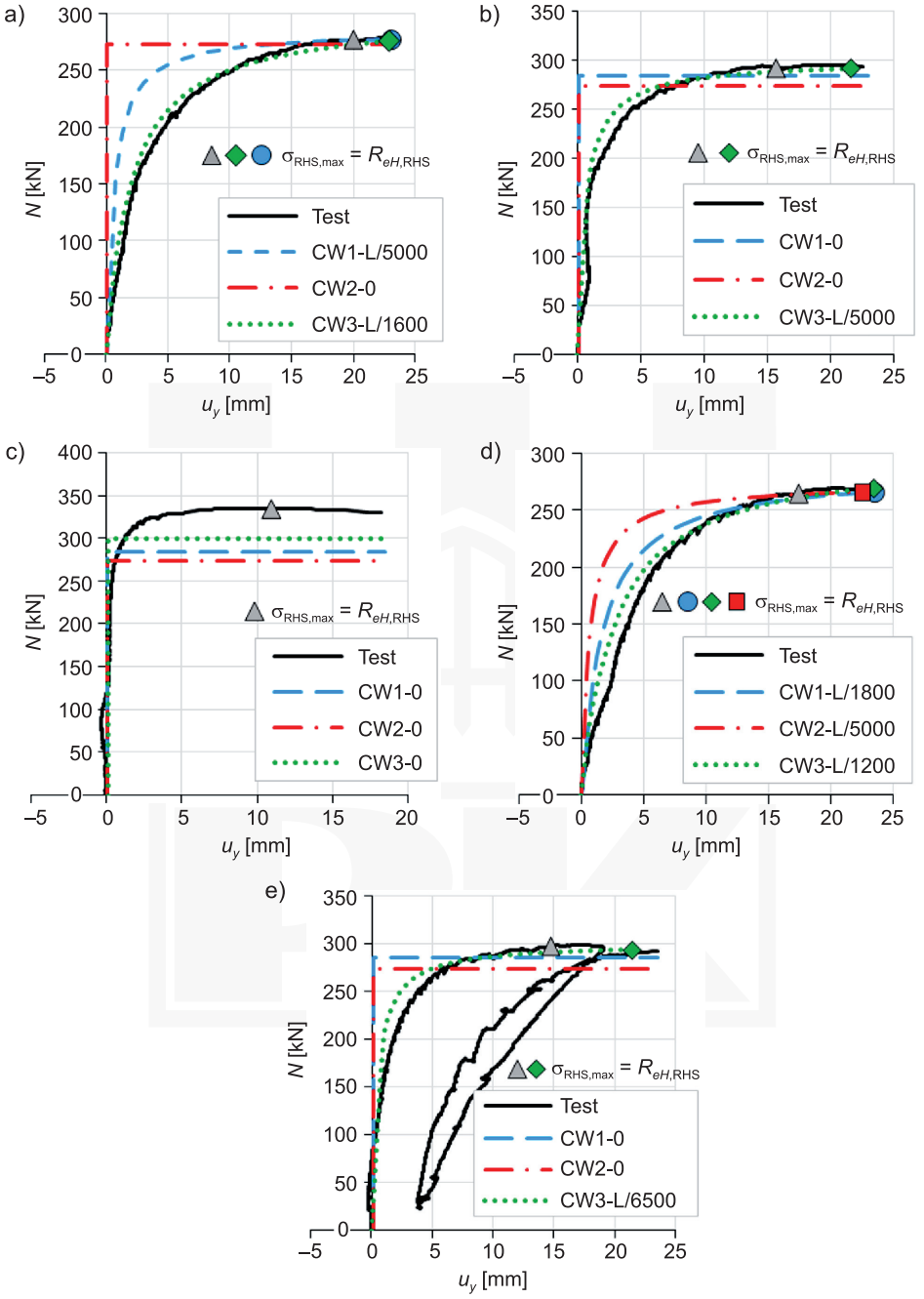

Fig. 24. Comparison of $N - u_y$ relationships measured and obtained in the analytical solution for test elements: a), b), c), d) and e) – Bz-1 to Bz-5, respectively

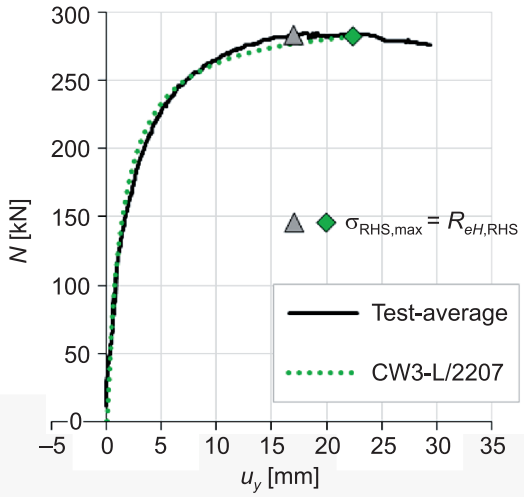

Fig. 25. Relationships $N - u_y$: measured and obtained analytically for the average amplitude a_y

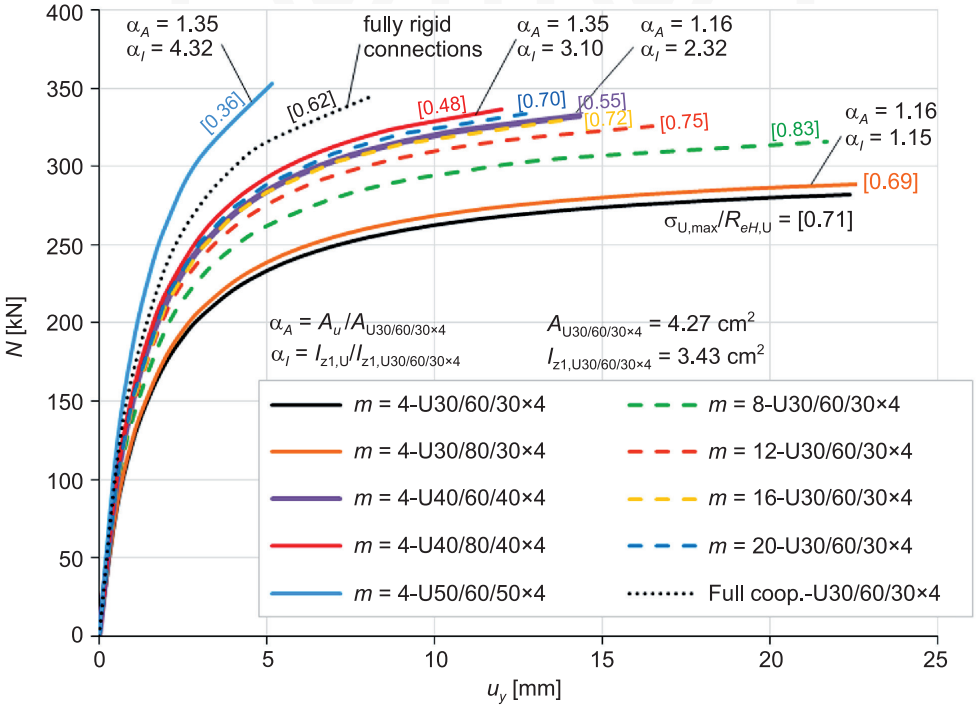

Fig. 26. Relationships $N - u_y$ obtained in the parametric analysis (description in the text)

– the buckling resistance of the column with U40/60/40×4 sections and only eight joints (m = 4) of the branches is comparable to the one, calculated for the column with U30/60/30×4 sections and forty joints (m = 20),
– the carrying capacity of the column with U50/60/50×4 sections and eight flexible joints (m = 4) constitutes approx. 102% of the carrying capacity of the column with U30/60/30×4 sections but with perfectly rigid joints (e.g. welded connections of the branches),
– an increase in both: the secondary moment of area $I_{z1,U}$ (α_I ratio) of the strengthening branches and the number m of the joints is accompanied by the decreasing strenuous of the strengthening U-shape branches ($\sigma_{U,max}/R_{eH,U}$ ratio in the square brackets).

9. Conclusions

A four-stage research programme including experimental and theoretical studies was carried out.

The first stage of the programme covered the shearing tests for single-cut joints with BOM-R16-4 fasteners (six test elements). The tests proved that the tested joints exhibit structural properties that are similar to the properties for the joints with standard 8.8 grade M16 bolts. High values of both shear and bearing resistance as well as a great stiffness and deformation capacity in the bearing constitute advantages over other popular blind fasteners such as screws or rivets.

In the second stage of the research programme, five three-branched columns in compression were tested. Results of the tests demonstrated the efficiency of the performed strengthening of the tubular bar using two U-shape sections connected to the strengthened bar using eight lap joints with BOM-R16-4 fasteners. The design buckling resistance of the tested columns was noticeably higher than that for the tubular bar before strengthening. At the same time, due to the flexibility of the joints of the branches, the design buckling resistance of the tested columns was visibly lower than that calculated for the column with perfectly rigid joints.

Within the third stage of the programme, validity of the proposed theoretical model describing the behaviour of the tested columns was proved. However, attention should be paid to the simplifying assumptions made in the analytical solution which limit the scope of the applications of the model.

Results of parametric studies performed within the fourth stage of the programme showed that striving both to increase the secondary moment of the area of the strengthening branches and to reduce the number of joints of the strengthened bar and the strengthening branches is a cost-effective way to gain efficiency of the strengthening process. Due to the high price of labour, a major part of the strengthening cost has a direct relationship with the fabrication of connections of the branches. Therefore, it is better to save labour at the expense of material – admission to only partial strenuous of strengthening branches.

Within the scope of further research, work on the development of a numerical model based on FEM will be undertaken. This model will not only enable the analyses of built-up columns with various geometrical and strength parameters but also the arbitrary arrangement

of joints of cooperating branches. It will be also possible to take into account the influence of the existing states of load and imperfections in the bar which is to be strengthened on the buckling resistance of the built-up member after strengthening.

Results of the performed research programme proved that BOM blind fasteners may be an efficient and cost-effective alternative to standard bolts in lap connections of strengthened bars with closed rectangular cross-section and strengthening branches with open cross--sections. It may be also stated that due to the relatively small labour consumption, the described strengthening method meets the demands of sustainable development in building industry.

This publication was supported by project 11.11.100.197/AS.

References

[1] Dawood M., Rizkalla S., *Environmental durability of a CFRP system for strengthening steel structures*, Construction and Building Materials, Vol. 24, 2010, 1682-1689.

[2] Shaat A., Fam A., *Axial loading tests on short and long structural steel columns retrofitted using carbon fibre reinforced polymers*, Canadian Journal of Civil Engineering, Vol. 33(4), 2006, 458-470.

[3] Lanier B., Schnerch D., Rizkalla S., *Behavior of steel monopoles strengthened with high-modulus CFRP materials*, Thin-Walled Structures, Vol. 47, 2009, 1037-1047.

[4] Piekarczyk M., *Zastosowanie technologii klejenia w budowlanych konstrukcjach metalowych*, Wydawnictwo Politechniki Krakowskiej, Kraków 2013.

[5] Teng J.G., Yu T., Fernando D., *Strengthening of steel structures with fiber-reinforced polymer composites*, Journal of Constructional Steel Research, Vol. 78, 2012, 131-143.

[6] Żółtowski W., Wierzbicki S., Król P., Witkowski J., *Błedne założenia projektowe przyczyną awarii konstrukcji hali,* XXIII Konferencja Naukowo-Techniczna Awarie Budowlane, Szczecin--Międzyzdroje, 2007, 699-706.

[7] Di Lorenzo G., Landolfo R., *Shear experimental response of new connectiong systems for cold--formed structures*, Journal of Constructional Steel Research, Vol. 60, 2004, 561-579.

[8] Mucha j., Witkowski W., *The expermiental analysis of the double joint type change effect on the joint destruction process in uniaxial shearing test*, Thin-Walled Structures, Vol. 66, 2013, 39-49.

[9] Becque J., Rasmussen K.J.R., *Experimental investigation of the interaction of local and overall buckling of stainless steel I-columns*, Journal of Structural Engineering, Vol. 135(11), 2009, 1340-1348.

[10] Stone T., La Boube R.A., *Behavior of cold-formed steel built-up sections*, Thin-Walled Structures, Vol. 43, 2005, 1805-1817.

[11] Zhang J.H., Young B., *Compression tests of cold-formed steel I-shaped open sections with edge and web stiffeners*, Thin-Walled Structures, Vol. 52, 2012, 1-11.

[12] Bolte W.G., LaBoube R.A., *Behavior of curtain wall stud to track connections*, Thin-Walled Structures, Vol. 42, 2004, 1431-1443.

[13] LaBoube R.A., Yu W.W., *Recent research and developments in cold-formed steel framing*, Thin--Walled Structures, Vol. 32, 1998, 21-39.

[14] ALCOA Fastening Systems, *The Huck Product Range – BOM*, (online) homepage: http:// pdf.directindustry.com/pdf/huck-r/the-huck-r-product-range/34809-323383.html (access: 07.07.2015).

[15] Wuwer W., *Podatne połączenia na sworznie jednostronne w prętowych konstrukcjach cienkościennych*, Wydawnictwo Politechniki Śląskiej, Gliwice 2006.
[16] Wuwer W., *The behaviour and design of lap-joints in thin-walled bar constructions*, Advanced Steel Construction an International Journal, Vol. 4(1), 2008, 59-83.
[17] Wuwer W., *Flexible nodes in calculations of thin-walled structures*, 3rd International Conference on Steel Structures Eurosteel, Coimbra, 2002, 1189-1198.
[18] Swierczyna S., *Nośność i sztywność jednociętych połączeń sworzniowych w konstrukcjach z kształtowników giętych*, Doctoral thesis, (online) homepage: http://delibra.bg.polsl.pl/Content/1317/calosc_rozprawa.pdf (access: 07.07.2015).
[19] Swierczyna S., Wuwer W., *Thin-walled latticed frame with semi-rigid bolted joints*, 12th International Conference on Steel Structures Progress in Steel and Composite Structures, Wrocław, 2011, 256-257.
[20] Swierczyna S., Wuwer W., *Evaluation of bearing resistance of blind bolt lap joints*, 7th European Conference on Steel and Composite Structures Eurosteel, Naples, 2014, 256-257.
[21] Słowiński K., *Badanie nośności ściskanych osiowo elementów bliskogałęziowych z podatnymi połączeniami*, Doctoral thesis, Gliwice 2013.
[22] PN-EN ISO 6892-1 Metale – Próba rozciągania – Część 1: Metoda badania w temepraturze pokojowej.
[23] ECCS TC7 TWG 7.10 Connections in cold-formed structures – The testing of connections with mechanical fasteners in steel sheeting and sections.
[24] PN-EN 1990 Eurokod – Podstawy projektowania konstrukcji.
[25] PN-EN 1993-1-8 Eurokod 3 – Projektowanie konstrukcji stalowych – Część 1–8: Projektowanie węzłów.
[26] Galambos T.V., *Guide to stability design criteria for metal structures 5th edition*, John Wiley & Sons, New York 1998.
[27] Krentz J.St., Haller W., *Zur Einstufung von rechteckigen und quadratischen hohlprofilen in DIN 18800*, Der Stahlbau, Vol. 57, 1988, 129-134.
[28] PN-EN 1993-1-1 Eurokod 3 – Projektowanie konstrukcji stalowych – Część 1–1: Reguły ogólne i reguły dla budynków.
[29] Grzymkowski R., Kapusta A., Kuboszek T., Słota D., *Mathematica 6*, Wydawnictwo Pracowni Komputerowej Jacka Skalmierskiego, Gliwice 2008.